Solar Energy Vol. 51, No. 5, pp. 317–325, 1993
Printed in the U.S.A.

0038-092X/93 $6.00 + .00

NEW HIGH-FLUX TWO-STAGE OPTICAL DESIGNS FOR PARABOLIC SOLAR CONCENTRATORS

ROBERT P. FRIEDMAN,* J. M. GORDON,* and HARALD RIES**
*Center for Energy and Environmental Physics, Jacob Blaustein Institute for Desert Research, Ben-Gurion University of the Negev, Sede Boqer Campus 84993, Israel, and The Pearlstone Center for Aeronautical Engineering Studies, Department of Mechanical Engineering, Ben-Gurion University of the Negev, Beersheva, Israel, **Center for Energy Research and Environmental Studies, Weizmann Institute of Science, Rehovot 76000, Israel

Abstract—We present a new two-stage optical design for parabolic dish concentrators that can realistically attain close to 90% of the thermodynamic limit to concentration with practical, compact designs (e.g., at parabola rim half-angles of around 45°). For comparison, the parabolic dish-plus-compound parabolic concentrator secondary design, at this rim angle, achieves no more than 50% of the thermodynamic limit. Our new secondary concentrator is tailored to accept edge rays from the parabolic primary, and incurs less than one reflection on average. It necessitates displacing the absorber from the parabola's focal plane, along the concentrator's optic axis, toward the primary reflector, and constructing the secondary between the absorber and the primary. The secondary tailored edge-ray concentrators described here create new possibilities for building compact, extremely high flux solar furnaces and/or commercial parabolic dish systems.

1. INTRODUCTION

Attaining the thermodynamic limit to optical concentration for solar collectors, while maintaining reasonably compact devices, requires the use of two-stage optical designs[1–3]. The primary is a focusing concentrator, selected for compactness and the associated ease of tracking and mechanical stabilization. Without secondary concentration, primaries such as parabolic reflectors fall short of the thermodynamic limit typically by a factor of 4 for 3-D (point-focus) systems[1–3].

Nonimaging secondaries are best suited to boost overall concentration significantly. One type is the compound parabolic concentrator (CPC)[1–3]. Another type is the hyperbolic concentrator commonly referred to as the "trumpet"[1,4,5]. Both CPCs and trumpets can in principle increase overall concentration to the thermodynamic limit, but with important qualifications.

The CPC is well suited to the flux map from focusing primaries only at high ratios of focal length to diameter f/D of the primary, also equivalently cited as small rim half-angles ϕ_{max} (see Fig. 1). Hence two-stage designs that can approach the thermodynamic limit are unwieldy in size and poorly suited to practical large-scale solar installations, such as solar furnaces, process heat production, and power generation. At f/D ratios suitable to practical dimensions, e.g., $\phi_{max} \gtrsim 40°$, the concentration of two-stage designs with CPC secondaries is no better than half the thermodynamic limit. The lack of suitability of the CPC for the particular flux map produced by the focusing primary is expanded upon in Appendix A.

The trumpet design calls for keeping the absorber in the focal plane and having the trumpet reflectors extend from the absorber to the primary, hence shading the entire primary. Truncating the trumpet to an extent that permits reasonable collection efficiency (i.e., acceptable shading losses) severely reduces achievable concentration—again, typically to no better than half the thermodynamic limit for practical solar concentrators[1,4,5].

Recently, a new concept in secondary concentration was proposed and developed for Fresnel reflector primaries: the tailored edge-ray concentrator (TERC), in which the secondary is fashioned to collect the extreme rays from each point on the primary[6]. The purpose of this paper is to craft this new methodology to parabolic concentrators. We will demonstrate that for admissibly compact two-stage solar concentrators, the parabolic dish-plus-TERC design can achieve close to 90% of the thermodynamic limit, thereby representing an improvement of about a factor of 1.8 in overall concentration relative to the (3-D) parabola-plus-CPC or parabola-plus-trumpet designs.

Our attention here is restricted to paraboloidal (dish) primaries, for a number of reasons. First, for large-scale solar applications where lenses are impractical and reflective optics are used, the parabolic primary offers higher concentration than other alternatives, such as Fresnel reflectors (often called solar towers or central receivers). Second, achieving high solar flux requires 3-D (point focus) rather than 2-D (line focus) concentrators. Third, new two-stage CPC-based solutions were recently devised that can reach 90% of the thermodynamic limit (in 2-D) with impressively compact, practical designs[7]. However, the rotationally symmetric 3-D versions of these configurations suffer from excessive skew ray rejection, and therefore fall far short of the thermodynamic limit. Fourth, the results derived here for 3-D systems are easily applicable to corresponding 2-D designs for any flat or convex (e.g., tubular) absorber.

In section 2, we review fundamental concepts on the maximum concentration achievable with two-stage designs, and the suitability of CPC secondaries for the particular flux map generated by the parabolic primary. In section 3, we describe how the TERC formalism is

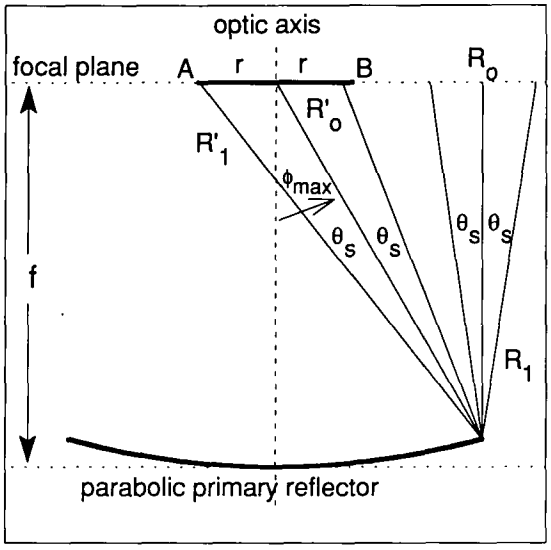

Fig. 1. Schematic 2-D cross section of parabolic concentrator with flat one-sided absorber AB. Parabolic focal length = f. ϕ_{max} = rim half-angle. Incident solar light cone subtends effective half-angle of θ_s. Relative to actual solar designs, θ_s is grossly exaggerated in order to show primary and absorber on the same scale. Incident RHS edge ray R_1 is reflected to ray R'_1, to the LHS edge of the absorber (point A). Incident ray R_0 is reflected to ray R'_0, to the parabola's focal point. The smallest absorber radius r required to collect all incident rays in the focal plane is always larger than the thermodynamic limit. A CPC secondary with entrance aperture diameter 2 r would be placed in the focal plane, with a reduced-size absorber behind it (away from the primary).

applied to parabolic primaries, specifically: (a) the optimal displacement of the absorber from the nominal focal plane; (b) the procedure for calculating the secondary reflectors; and (c) geometric limitations to the TERC design. In section 4, quantitative expression is given to the concentration and collection efficiency that can be reached with practical, relatively compact parabolic dish-plus-*truncated* TERC designs. Section 5 is a discussion of the significance of our results.

2. MAXIMUM CONCENTRATION WITH PARABOLIC DISH PRIMARIES

A 2-D cross section of the solar concentrator is shown in Fig. 1. The 3-D system is obtained by rotation about the concentrator's optic axis. The *effective* solar half angle θ_s is assumed to be known. It represents the solar disk size *as perceived at the absorber,* and is comprised of: the finite size of the solar disk (typically 0.0047 radian); atmospheric low-angle scattering; tracking and mirror contour errors; and collector misalignments. Many analyses of solar concentrators present illustrative calculations for $\theta_s = 0.0047$ radian. However no concentrator will be free of optical errors, so that the magnitude of θ_s for properly installed systems is typically a few tenths of a degree. Toward offering conservatively realistic illustrative calculations, we adopt the value $\theta_s = 0.010$ radian in the solved examples below.

We stress that the relative dimensions in Fig. 1 are purposely drawn far out of proportion relative to actual designs in order to show clearly details of the absorber *and* placement of the primary. Realistic solar concentrators will have $\theta_s \ll \phi_{max}$, and will have a much greater focal length compared to absorber size than in Fig. 1.

The derivation below of fundamental bounds on optical concentration is presented for both 2-D and 3-D systems. Whereas rigorous, analytic results for concentration *and* collection efficiency (fraction of incident rays that reach the absorber, ignoring reflector absorptive losses) can be obtained in 2-D, no such generalization is possible for the corresponding 3-D concentrator due to the partial rejection of skew rays. We can, however, place analytic bounds on the properties of the 3-D concentrator and then perform a (3-D) ray-trace simulation to determine the precise degree of deviation from ideal behavior.

To appreciate several basic aspects of achievable concentration, it is instructive to calculate the étendue (optical throughput) $\mathscr{E}$ of radiation reflected by the parabolic primary, with étendue defined as[1]

$$\mathscr{E} = \int\int d\mathscr{V} \, d\mathscr{X} \tag{1}$$

where $d\mathscr{V}$ = differential view factor (sometimes called projected angle in 2-D and projected solid angle in 3-D) of a pencil of rays striking a point; and $d\mathscr{X}$ = differential space volume element, which is an interval length in 2-D and an area element in 3-D. The thermodynamic limit to concentration can be calculated rigorously from conservation of étendue.

At any point on the parabola, the view factor of the sun is

$$\int d\mathscr{V} = v \cos(\phi/2) \tag{2}$$

where ϕ is the angular coordinate of a given point on the parabola, measured relative to the negative ordinate; and v is the view factor at solar zenith,

$$v = v_2 = 2 \sin(\theta_s) \quad \text{2-D} \tag{3a}$$

$$v = v_3 = \pi \sin^2(\theta_s) \quad \text{3-D.} \tag{3b}$$

The spatial coordinates are

$$\mathscr{X} = \mathbf{X}(\phi) \quad \text{2-D} \tag{4a}$$

$$\mathscr{X} = \pi[\mathbf{X}(\phi)]^2 \quad \text{3-D} \tag{4b}$$

where

$$\mathbf{X}(\phi) = 2f \tan(\phi/2) \tag{4c}$$

is the shortest distance from the parabola's optic axis to a given point on the parabola; the parabola aperture diameter at any point ϕ is $2\mathbf{X}(\phi)$; and f = parabola focal length.

It then follows that the étendue is

$$\mathscr{E}_{2\text{-D}}(\phi) = 4v_2 f \tan(\phi/2) \quad \text{2-D} \quad (5a)$$

$$\mathscr{E}_{3\text{-D}}(\phi) = 4\pi v_3 f^2 \tan^2(\phi/2) \quad \text{3-D.} \quad (5b)$$

Maximum concentration corresponds to minimum absorber area, $\mathscr{A}_{\text{abs-min}}$ and maximum view factor, the latter being 2 in 2-D and π in 3-D. With eqns (5a) and (5b) (evaluated at $\phi = \phi_{\max}$), one then obtains

$$\mathscr{A}^{\text{2-D}}_{\text{abs-min}} = \mathscr{E}_{2\text{-D}}/2 = 2v_2 f \tan(\phi_{\max}/2)$$
$$(= \text{absorber diameter}) \quad (6a)$$

$$\mathscr{A}^{\text{3-D}}_{\text{abs-min}} = \mathscr{E}_{3\text{-D}}/\pi = 4v_3 f^2 \tan^2(\phi_{\max}/2)$$
$$(= \text{absorber disc area}). \quad (6b)$$

From eqns (6a) and (6b) follow the result that the thermodynamic limit to overall concentration C, defined as the ratio of aperture area to absorber area subject to the requirement that all incident rays be accepted, is

$$C^{\text{2-D}}_{\max} = 1/\sin(\theta_s) \quad (7a)$$

$$C^{\text{3-D}}_{\max} = 1/\sin^2(\theta_s). \quad (7b)$$

However eqns (7a) and (7b) are *general* statements of maximum concentration that are *not* restricted to the particular concentrators considered here[1]. As noted above, many analyses illustrate maximum concentration with the value $\theta_s = 0.0047$ radian, for which $C^{\text{3-D}}_{\max}$ is 45,000. This, however, ignores concentrator optical errors. In the spirit of more realistic illustrative examples, we have conservatively chosen $\theta_s = 0.010$ radian, for which $C^{\text{3-D}}_{\max} = 10{,}000$. Whatever the effective solar disk size θ_s may be, eqns (7a) and (7b) represent the thermodynamic limit to concentration for that value.

Equations (6a) and (6b) also permit us to place a lower bound on skew ray rejection for the 3-D concentrator that is the rotationally symmetric version of the 2-D device. For the case of the parabolic primary,

$$\mathscr{A}^{\text{3-D}}_{\text{abs-min}} = (\pi/4)[\mathscr{A}^{\text{2-D}}_{\text{abs-min}}]^2. \quad (8)$$

This means that skewness conservation does not exclude the possibility that the rotationally symmetric 3-D concentrator will achieve maximum concentration, i.e., that there will be no skew ray rejection. This is *not* the case, for example, for the Fresnel reflector, where it was shown that the lack of equality in eqn (8) implies a non-negligible minimum degree of skew ray rejection[6]. The equality [eqn (8)] does not, however, guide us to a solution for the problem of the design of the second-stage concentrator that will attain maximum concentration; it only indicates that its existence cannot be excluded. The CPC secondary rejects between 1–5% of skew rays, depending on parabola rim angle, with the higher skew ray rejection corresponding to lower rim angles[1].

One example of a secondary that in principle can reach the thermodynamic limit is the trumpet concentrator. As noted above, however, a full trumpet totally shades the primary, and for practical concentrators that necessitate compactness and high collection efficiency, the concentration boost provided by an appropriately truncated trumpet still falls short of the thermodynamic limit by around a factor of two[1,4,5].

To appreciate quantitatively the overall concentration C of the parabolic dish-plus-CPC design, including shading of the primary by the secondary, we express C in terms of ϕ and θ_s only:

$$C = \frac{\sin^2(\phi_{\max})}{\sin^2(\theta_s)\tan^2(\phi_{\max} + \theta_s)} - \frac{1}{\sin^2(\phi_{\max} + \theta_s)}. \quad (9)$$

Equation (9) is plotted in Fig. 2 for the specific value $\theta_s = 0.010$ radian. Equation (9) does not include the 1–5% loss due to skew ray rejection. C is maximized at $\phi_{\max} \approx 12°$, i.e., f/D $\approx$ 2.4. These values are close to the parameters selected by Gleckman *et al.* in their laboratory-scale concentrator for attaining flux levels close to the thermodynamic limit (although they employed a refractive dielectric secondary, rather than a reflective secondary, in order to increase concentration). Whereas a parabolic dish-plus-CPC designed for $\phi_{\max} = 12°$ may be the configuration that maximizes concentration (Fig. 2), and attains 87% of $C_{\max}$ (a figure that is reduced to 83% when skew ray rejection is accounted for) at $\theta_s = 0.010$ radian, the high f/D ratio renders it impractical for large-scale solar installations. At practical rim half-angles of around $\phi_{\max} = 45°$ (f/D = 0.6), overall concentration is no higher than 50% of $C_{\max}$.

3. THE TAILORED EDGE RAY CONCENTRATOR (TERC) SECONDARY

3.1 *Construction principle*

The guiding tenet of nonimaging optics is the edge-ray principle, which requires that extreme rays at the

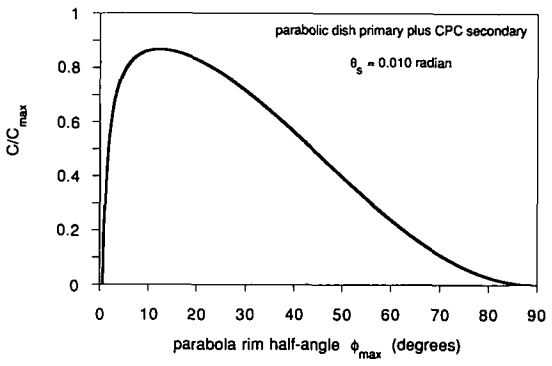

Fig. 2. Overall concentration C relative to the thermodynamic limit, $C_{\max} = 1/\sin^2(\theta_s)$, versus parabola rim half-angle $\phi_{\max}$ for parabolic dish-plus-CPC two-stage design, at $\theta_s = 0.010$ radian. Shading of the primary by the secondary is accounted for, but skew ray rejection is not. The latter is in the range 1–5% with larger skew ray rejection at smaller rim angles.

concentrator aperture must also be extreme rays at the absorber (extreme meaning tangent or edge). The TERC[6]adheres to the edge-ray principle: each point on the TERC reflector is required to reflect extreme rays from the incident solar light cone (from each point on the primary) to the opposite absorber edge, which mandates reflector slope. Additionally specifying the TERC's starting point, e.g., at the absorber plane, then completely determines the reflectors. Motivating the TERC construction from an analysis of the phase space of rays that reach the absorber plane is presented in Appendix A.

Given a parabolic primary, the design of a TERC necessitates displacing the absorber from the parabola's focal plane, along the optic axis, toward the primary (see Fig. 3a), in order to avoid the caustic formed by the edge rays falling between the primary and secondary reflectors. In Fig. 3a, as in Fig. 1, the relative dimensions are intentionally drawn out of proportion relative to actual designs (i.e., relatively large ratio of absorber diameter to parabola focal length), in order to clarify this point.

Consider the extreme rays of the solar light cone from the RHS of the primary (starting at $\phi = \phi_{max}$). In Figs. 1 and 3a, the incident RHS extreme ray R_1 is reflected to ray R'_1, and intersects the focal plane (on the LHS of the optic axis) at a radius r that is far greater than the radius of the minimum size absorber $\mathscr{A}^{2\text{-D}}_{abs\text{-}min}/2$:

$$r = \frac{2f\tan(\phi_{max}/2)\sin(\theta_s)}{\sin(\phi_{max})\cos(\phi_{max} + \theta_s)}. \qquad (10)$$

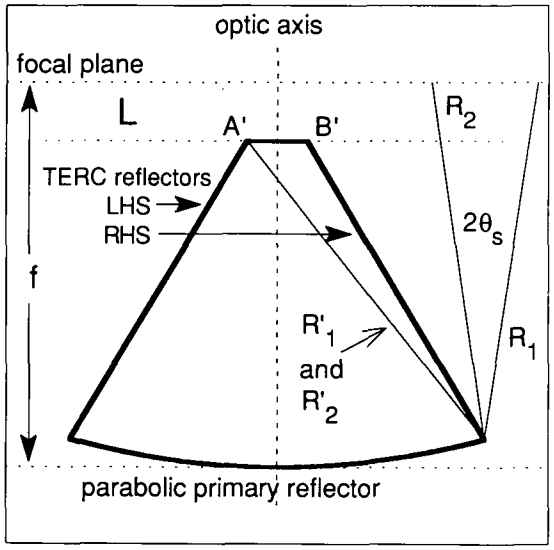

Fig. 3a. Illustration (2-D cross section) of displacement of absorber from parabola focal plane by distance L, and reduction to minimum-size absorber A'B'. As in Fig. 1, θ_s is grossly exaggerated in order to show primary and absorber on the same scale. Incident RHS edge ray R_1 from the parabola's rim is reflected to ray R'_1 to the LHS edge of the absorber (point A'). The slope of the LHS TERC reflector, which starts at point A', ensures that ray R'_1 is reflected to point B'. Ray R_2 (reflected to ray R'_2), and all incident rays between R_1 and R_2, are automatically accommodated by the TERC. TERC reflectors are shown fully extended to the primary.

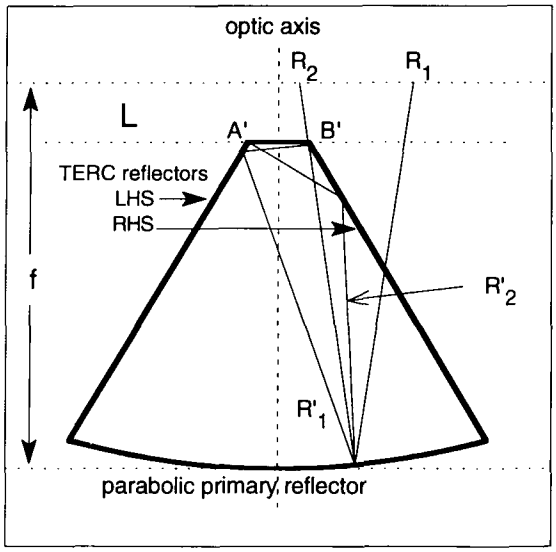

Fig. 3b. Illustration of TERC construction principle for rays reflected from an intermediate point on the parabolic primary. Notation as in Fig. 3a. Incident RHS edge ray R_1, reflected to ray R'_1, is reflected by the LHS TERC reflector to the opposite absorber edge (B'). For symmetry reasons, incident ray R_2, reflected to ray R'_2, is reflected by the RHS TERC reflector to the absorber edge A'. This ensures that all incident rays within the solar light cone of angular extent 2 θ_s (from R_1 to R_2) are accommodated.

One then moves the *minimum size* absorber out of the focal plane, along the optic axis, toward the primary, until the reflected edge ray R'_1 exactly strikes the LHS edge of the minimum-size absorber (point A' in Fig. 3a). From elementary geometry, this vertical displacement from the focal plane L is

$$L = 2f\tan(\phi_{max}/2) \times \left[\frac{1}{\tan(\phi_{max})} - \frac{1 + \sin(\theta_s)}{\tan(\phi_{max} + \theta_s)}\right]. \qquad (11)$$

The slope of the LHS TERC reflector (at its starting point, at the LHS absorber edge A') ensures that this edge ray is reflected to the opposite absorber edge (point B' in Fig. 3a). For the description of how the TERC is constructed, we first purposely ignore the fact that the TERC shades the primary, then illustrate the construction principle, and subsequently account for shading effects exactly.

The TERC construction principle is illustrated in Fig. 3b, to which we now refer. One moves along the parabola (to the left, $\phi < \phi_{max}$) and determines TERC reflector slope such that the RHS edge ray R_1 of the solar light cone from each point on the primary, reflected to ray R'_1, hits the LHS TERC reflector and, after a single reflection, reaches the opposite absorber edge (point B'). The construction principle ensures that all incident rays within the solar light cone of angular extent $2\theta_s$ (from R_1 to R_2) are accommodated. The construction ceases when the LHS TERC reflector reaches the LHS rim of the primary (at $\phi = -\phi_{max}$).

By symmetry, the RHS TERC reflector is the mirror image of the LHS, and the TERC is then uniquely determined. Consequently incident ray R_2, reflected to ray R_2', hits the RHS TERC reflector and, after a single reflection, reaches the absorber at its other edge A'. Similarly in Fig. 3a, at the extreme (rim) point on the primary, the LHS incident edge ray R_2 will also be reflected by the RHS TERC reflector to absorber edge A'.

The full or untruncated TERC is clearly useless since it shades the entire primary. However, as will be demonstrated in section 4, highly truncated, compact TERCs can achieve almost 90% of C_{max} (at maximum collection efficiency). Sample scale drawings of truncated TERCs (truncated in order to show clearly absorber size and reflector shape) are shown in Fig. 4, with one unit being the radius of the minimum size absorber, and all three TERCs in Fig. 4 being drawn for the same absorber size.

The TERCs in Fig. 4 are remarkably close to being cones (V-troughs in 2-D), but actually are *not* cones. This is evidenced in Fig. 5—a plot of reflector slope versus TERC depth—which would have strictly constant curves (horizontal lines) for cone concentrators.

3.2 *Range of validity*

The geometry of the parabolic primary limits the strict validity of the TERC construction principle to the range $\phi_{max} < 36.6°$ (see Appendices A and B for a derivation and for the graphical interpretation in phase space). The limiting ϕ_{max} value depends on θ_s, and the 36.6° figure corresponds to $\theta_s = 0.010$ radian. One way to understand this constraint is that when $\phi_{max} > 36.6°$, the smallest radius intercepted in the absorber plane from a reflected solar light cone emanates from an intermediate point on the primary ($\phi < \phi_{max}$) rather than from the *rim* point ($\phi = \phi_{max}$). The prescribed TERC construction then reaches the primary at some $\phi < \phi_{max}$, which indicates an inconsistent solution (see Appendix B).

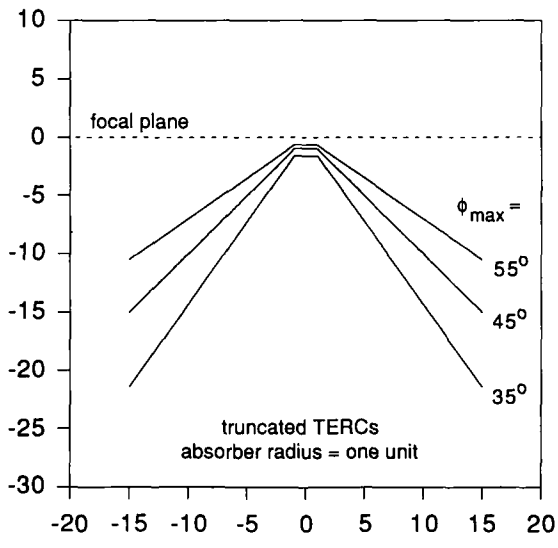

Fig. 4. Scale drawings, 2-D cross sections of truncated TERCs, with one unit equal to the absorber radius, for $\phi_{max} = 35°$, 45°, and 55°. The TERCs are truncated (arbitrarily) to an entrance aperture equal to 15 times the diameter of the minimum size absorber, and all three TERCs have the same absorber size.

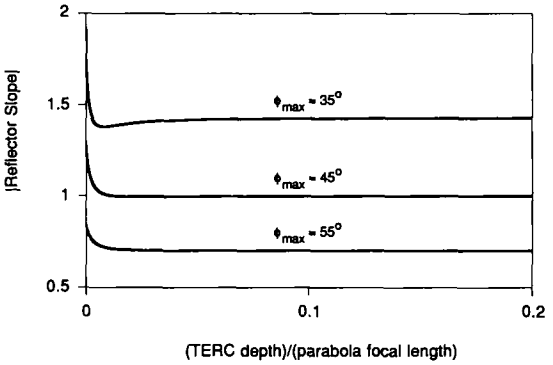

Fig. 5. Reflector slope versus TERC depth (relative to parabola focal length). Were the TERCs actually cones (V-troughs in 2-D), the curves would be horizontal lines.

The TERC will fail to collect all rays from the primary, unless some modification is introduced. An analogous limitation was found for the Fresnel reflector primary [6], where the rigorous TERC construction is constrained to $\phi_{max} < 49.6°$. Designs for $\phi_{max} > 36.6°$ *can* closely approach the thermodynamic limit (the deviation increasing with ϕ_{max}) and are of considerable practical interest due to their relatively low f/D ratios. Hence, we proceed to describe the design of TERCs for large rim angles (this section), and to evaluate achievable concentration at maximum collection efficiency, and collection efficiency at maximum concentration (the following section).

The maximum rim half-angle for which the TERC construction can strictly be used can be calculated from basic geometry as the solution ϕ^* to the equation:

$$0 = 2\sin(\phi^*)\{1 + \sin(\theta_s)\} - \sin(2\phi^* + 2\theta_s) - 2\tan(\phi^*/2)\sin^2(\phi^* + \theta_s). \quad (12)$$

When $\phi_{max} > \phi^*$, maximum collection efficiency can be maintained if the absorber is oversized (i.e., if concentration is sacrificed). To determine the smallest absorber size for which a consistent TERC solution can be generated, one starts with the minimum size absorber [eqn (6a)], gradually increases absorber size, and for each absorber size applies the TERC construction principle until the absorber is just large enough to yield a solution for the TERC reflector that terminates at the primary at $\phi = \phi_{max}$ (i.e., a self-consistent solution). For each absorber diameter selected, say, a factor of Q larger than the minimum-diameter absorber, the displacement of the absorber from the focal plane must be changed accordingly [from L in eqn (11) to a new value L']:

$$L' = 2f\tan(\phi_{max}/2) \times \left[\frac{1}{\tan(\phi_{max})} - \frac{1 + Q\sin(\theta_s)}{\tan(\phi_{max} + \theta_s)}\right]. \quad (13)$$

In the following section, we analyze the achievable concentration from practical, *truncated* TERCs. Cases with $\phi_{max} > \phi^*$ are based on the compromise design described immediately above, as are the TERCs plotted in Fig. 4.

4. QUANTITATIVE EXAMPLES OF PRACTICAL TERC DESIGNS

Any practical, compact design requires severe truncation of the TERC, in order to avoid excessive shading of the primary. Fortunately, the TERC's outermost reflector sections provide relatively little concentration, so that high degrees of truncation result in only modest losses in concentration. Independent of practical considerations, the TERC has an *energetically* optimal degree of truncation. With no truncation, the TERC completely shades the primary, so effective concentration is zero. At total truncation, only the parabolic primary with displaced absorber (without TERC) remains. Overall concentration is maximized at some intermediate degree of truncation, which depends on ϕ_{max} (and θ_s) only.

TERC design can be geared toward requiring either maximum collection efficiency (at minimum sacrifice in concentration), or stipulating maximum concentration (at minimum sacrifice in collection efficiency).

First consider the case of demanding maximum collection efficiency. Assume that ϕ_{max} is given (based on practical and/or mechanical constraints). A truncated TERC that will collect all rays from the primary must therefore be designed for a fictitious, oversized value of ϕ_{max}, ϕ_{max}(oversized), and truncated so as to accommodate all rays incident from the actual primary. The attainable concentration in this case is plotted in Fig. 6, for several values of ϕ_{max} as a function of TERC depth. Each point on a given curve in Fig. 6 corresponds to the smallest absorber size commensurate with the TERC construction principle at that particular

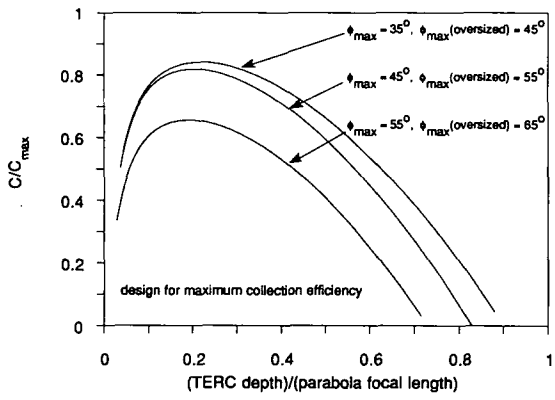

Fig. 6. Overall concentration C relative to the thermodynamic limit C_{max} versus TERC depth (relative to primary focal length), for truncated TERCs designed for maximum collection efficiency. The actual primary rim half-angle ϕ_{max} and the fictitious oversized rim half-angle ϕ_{max}(oversized) for which TERC constructions have been generated are: (a) $\phi_{max} = 35°$, ϕ_{max}(oversized) = 45°; (b) $\phi_{max} = 45°$, ϕ_{max}(oversized) = 55°; (c) $\phi_{max} = 55°$, ϕ_{max}(oversized) = 65°.

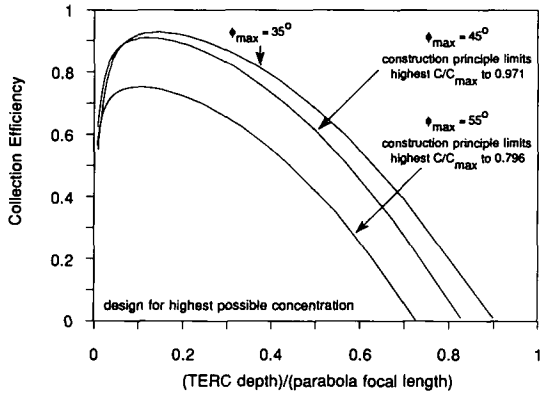

Fig. 7. Collection efficiency versus TERC depth (relative to primary focal length), for truncated TERCs designed for maximum concentration. ϕ_{max} = 35°, 45°, and 55°.

degree of TERC truncation, and includes shading of the primary by both TERC and absorber.

For the alternative design of requiring maximum concentration at minimum sacrifice in collection efficiency (again assuming ϕ_{max} is fixed), one designs the TERC as detailed in section 3 and implements truncation via gradual removal of the outermost reflector sections. Figure 7 shows collection efficiency (including shading losses) as a function of the degree of TERC truncation for several values of ϕ_{max}. When $\phi_{max} > \phi^*$ = 36.6°, the concentration is taken to be the largest value permitted by the modified TERC construction principle described in subsection 3.2. Note that the optimum degree of TERC truncation in this case is different from that determined from the maximum collection efficiency design (Fig. 6).

To check the effect of skew-ray rejection on TERC collection efficiency, we performed a 3-D ray trace simulation for designs with ϕ_{max} in the range 30–60°. Skew ray rejection decreases as the degree of truncation increases and as ϕ_{max} increases. For all the truncated TERCs considered here, skew ray rejection turns out to be less than 1%. Hence the quantitative studies presented here for truncated TERCs, which are based on analytic calculations that ignore skew ray losses, are accurate to within better than 1%.

5. DISCUSSION

The new two-stage optical design of parabolic dish-plus-TERC secondary presented here creates a new capability: reaching close to 90% of the thermodynamic limit to concentration with *practical, compact* configurations, i.e., small f/D ratios. Although laboratory-scale two-stage designs with parabolic primaries and CPC secondaries that achieve concentration ratios in excess of 80% of the thermodynamic limit have been built[8], they are inherently limited to small parabola rim angles (large f/D ratios), and hence may be viewed as impractical for large-scale solar energy applications such as solar furnaces, process heat production, and power generation. At parabola rim half-angles of around 45°, parabolic primaries with CPC or trumpet

secondaries can attain concentrations of no more than 50% of the thermodynamic limit.

The TERC is designed according to the edge-ray principle of nonimaging optics[1,6]so as to accommodate the particular flux produced by the primary. It also requires the fundamental modification of displacing the absorber from the focal plane, toward the primary, and constructing the secondary between the absorber plane and the parabola.

The full TERC construction requires its extending from the absorber to the primary, which is clearly unrealistic. Only considerably truncated TERCs can be compact enough for real applications. Due to shading of the primary by the TERC, there is an energetically optimal degree of truncation, which fortuitously corresponds to acceptably compact devices. This stems, in part, from most of the TERC's concentration deriving from the reflector sections closest to the absorber.

It turns out that even after all realistic optical losses are accounted for, compact truncated TERCs can attain close to 90% of the thermodynamic limit in concentration, at maximal collection efficiency. A 3-D ray trace simulation reveals that less than 1% of incident skew rays are rejected from the (truncated) 3-D TERCs analyzed here (that are rotationally symmetric versions of the corresponding 2-D TERCs). Furthermore, by virtue of its construction principle, the TERC incurs less than one reflection on average. The specific truncated TERCs considered here have an average number of reflections of around one-half. Therefore reflector absorptive losses should be acceptably small.

The TERC can be designed to maximize collection efficiency (at minimum sacrifice in concentration) or to maximize concentration (at minimum sacrifice in collection efficiency). Figures 6 and 7 show the performance limits of these TERC designs, the impact of TERC truncation, and the optimal degree of truncation. When the rim half-angle of the parabola exceeds around 37°, the TERC construction principle must be modified in a manner that sacrifices concentration, in order to ensure maximum collection efficiency. Fortunately, for rim half-angles in the practical range of around 45°, this loss of concentration is small. However, at rim half-angles above around 55°, the sacrifice in concentration becomes significant, and limits the value of the TERC secondary.

The emphasis in this paper has been on 3-D (parabolic dish), as opposed to 2-D (parabolic trough), concentrators, in part due to the desire to achieve the very high solar flux levels that are beneficial for solar furnaces, process heat production and power generation applications. However the TERC design principles developed here are equally easily applied to linear two-stage concentrators, for flat or convex (e.g., tubular) absorbers. The basic conclusions arrived at here for 3-D systems do not change markedly for 2-D systems with flat one-sided absorbers. However losses due to shading of the primary by the TERC are relatively larger in linear concentrators, and the fraction of maximum concentration (in 2-D) that can be reached is smaller than the corresponding result in 3-D.

With tubular absorbers, a large fraction of maximal concentration can be achieved up to far larger parabola rim angles than with flat absorbers (as is the case for the parabolic trough without a secondary). The value of the TERC relative to other secondary concentrators (in 2-D) is small since parabolic trough-plus-CPC secondary designs that can attain around 90% of the thermodynamic limit with compact devices have already been developed[7]. These high-concentration designs fail in 3-D, however (i.e., the rotationally symmetric version of the 2-D concentrator), due to excessive skew-ray rejection.

The cross section of the TERC turns out to be well approximated by a V-trough, although the reflectors are not linear, as demonstrated in Fig. 5. It is critical, however, that the TERC be used in conjunction with a specific optimal displacement of the absorber from the parabola focal plane. Deploying the TERC with the minimum size absorber in the *focal plane* will result in a significant fraction of incoming rays being rejected. It is therefore perhaps ironic to note that secondary V-troughs (in 2-D) and cones (in 3-D), conventionally viewed as inferior to CPCs as second stages for parabolic primaries, can actually be superior to CPCs *provided* the new absorber position is employed and the secondary opening angle is matched to the primary.

After the completion of the present paper we have learned that V-cones as secondary concentrators have been discussed in a recent work in an optimization approach[9]. The optimum found implies indeed moving the absorber out off the focal plane of the primary, which is in agreement with eqn (13). Their quantitative results concerning the efficiency, however cannot be directly compared to ours because the authors assumed a Gaussian distribution of the solar radiation, whereas our results hold for a pillbox distribution.

Acknowledgments—Harald Ries gratefully acknowledges the support of the Swiss Federal Office for Education and Science (B.B.W.), as well as the hospitality of the Center for Energy and Environmental Physics (Sede Boqer Campus, Israel) during part of this research.

NOMENCLATURE

- $\mathscr{A}$ absorber area (diameter in 2-D, disc area in 3-D)
- C overall geometric concentration ratio
- C_{max} thermodynamic limit to concentration
- CPC Compound Parabolic Concentrator
- $\mathscr{E}$ étendue (optical throughput)
- f parabola focal length
- f/D ratio of focal to diameter of the primary concentrator
- L vertical displacement of absorber plane from parabola focal plane
- L′ vertical displacement of absorber plane from parabola focal plane in constructing the TERC for the range $\phi_{max} > \phi^*$
- LHS left-hand side
- Q factor by which one increases absorber size in constructing the TERC for the range $\phi_{max} > \phi^*$
- RHS right-hand side
- TERC Tailored Edge-Ray Concentrator
- v view factor of sun at solar zenith
- $\mathscr{V}$ view factor
- X shortest distance from optic axis to a given point on the parabola
- $\mathscr{X}$ spatial coordinate
- ϕ angular coordinate along parabola

ϕ_{max} rim half-angle of parabola
ϕ^* parabola rim half-angle beyond which the prescribed TERC construction is not strictly valid
θ_s effective solar half-angle = acceptance half-angle of primary

REFERENCES

1. W. T. Welford and R. Winston, *High collection nonimaging optics*, Academic Press, San Diego (1989).
2. A. Rabl, Comparison of solar concentrators, *Solar Energy* **18**, 93–111 (1976).
3. A. Rabl, *Active solar collectors and their applications*, Oxford University Press, New York (1985).
4. J. O'Gallagher and R. Winston, Test of a "trumpet" secondary concentrator with a paraboloidal dish primary, *Solar Energy* **36**, 37–44 (1986).
5. D. Suresh, J. O'Gallagher, and R. Winston, Thermal and optical performance test results for compound parabolic concentrators (CPCs), *Solar Energy* **44**, 257–270 (1990).
6. J. M. Gordon and H. Ries, Tailored edge-ray concentrators (TERCs) as ideal second stages for Fresnel reflectors, *Applied Optics* **32**, 2243–2251 (1993).
7. M. Collares-Pereira, J. M. Gordon, A. Rabl, and R. Winston, High concentration two-stage optics for parabolic trough solar collectors with tubular absorber and large rim angle, *Solar Energy* **47**, 457–466 (1991).
8. P. Gleckman, J. O'Gallagher, and R. Winston, Concentration of sunlight to solar-surface levels using non-imaging optics, *Nature* **339**, 198–200 (1989).
9. U. Schoeffel and R. Sizmann, Optimization of two-stage concentrating systems for high temperature and high photon flux density applications, 1991 *Solar World Congress*, pp. 1893–1898, Pergamon Press, Oxford (1991).

APPENDIX A: SUITABILITY OF SECONDARY CONCENTRATORS FROM PHASE SPACE DIAGRAMS

Phase space refers to the spatial coordinates ($\mathscr{X}$) and view factors ($\mathscr{V}$) for the radiation traversing an optical system. The shape of the phase space region occupied by the radiation that reaches the absorber plane offers a graphic understanding of the suitability of a given secondary concentrator to the particular flux map produced by the primary.

First consider the case of the absorber lying in the parabola's focal plane. The design with a CPC secondary falls into this category, as the CPC entrance aperture becomes a virtual absorber in the focal plane, and the actual absorber is placed behind it, away from the primary. Figures 8a and 8b show the shape of the phase space region occupied by the radiation in the *absorber plane* for the 2-D and 3-D concentrators, respectively (for the specific case $\phi_{max} = 30°$). All lengths are expressed in units of the radius of the minimum-size absorber. The dependence of $\mathscr{X}$ and $\mathscr{V}$ on ϕ is:

$$\mathscr{X}(\phi) = P(\phi) \quad \mathscr{V}(\phi) = 2\sin(\phi) \quad \text{2-D} \qquad \text{(A1a)}$$

$$\mathscr{X}(\phi) = \pi P(\phi)|P(\phi)|$$

$$\mathscr{V}(\phi) = \pi \sin(\phi)|\sin(\phi)| \quad \text{3-D} \qquad \text{(A1b)}$$

where

$$P(\phi) = 2f\tan(\phi/2)\left[1 - \frac{\tan(\phi \pm \theta_s)}{\tan(\phi)}\right] \qquad \text{(A1c)}$$

with the ± corresponding to the LHS and RHS of the optic axis. In order to be able to compare cross sections through rotationally symmetric 3-D systems to 2-D systems, we weight $P(\phi)$ and $\sin(\phi)$ with their relative contributions, which in the 3-D case are $|P(\phi)|$ and $|\sin(\phi)|$, respectively.

Although the curve in Fig. 8a is rigorously correct, the curve in Fig. 8b should be viewed as only a qualitative representation, because it is a two-dimensional projection of what should properly be a four-dimensional plot. In 3-D, the directions of off-axis points do not possess rotational symmetry. However, the calculations of étendue in eqns (5a) and (5b) *are* rigorous.

In Figure 8, a vertical cross section represents the view factor at a particular location. Note that off-center points receive radiation from both sides of the primary reflector, but not from the central region. Because the radiation reflected from the primary and perceived in the absorber plane is symmetric both in position and direction, Fig. 8 exhibits symmetries about both the vertical and horizontal axes.

A CPC is *not* ideally suited to a parabolic primary because, in our notation, it transforms a rectangular region of phase space into a rectangular region of equal étendue with maximal view factor and therefore minimal area. For the particular shape depicted in Fig. 8, a CPC can be designed for the central region (marked with dotted lines). In this case, it achieves maximum concentration but loses all rays outside this central region. The collection efficiency then translates into the ratio of the areas of the small rectangular box to the étendue (area within the full curve).

Another possibility is to design the CPC for the (larger) rectangular region containing all the radiation (marked with broken lines in Fig. 8). In this case, no radiation is lost, but concentration is sacrificed. Intermediate solutions are also possible.

An ideal concentrator transforms *precisely* the phase space occupied by incoming radiation into a region of maximal view factor and minimal area. The flux density must then be constant (if the original incident radiance was constant). By

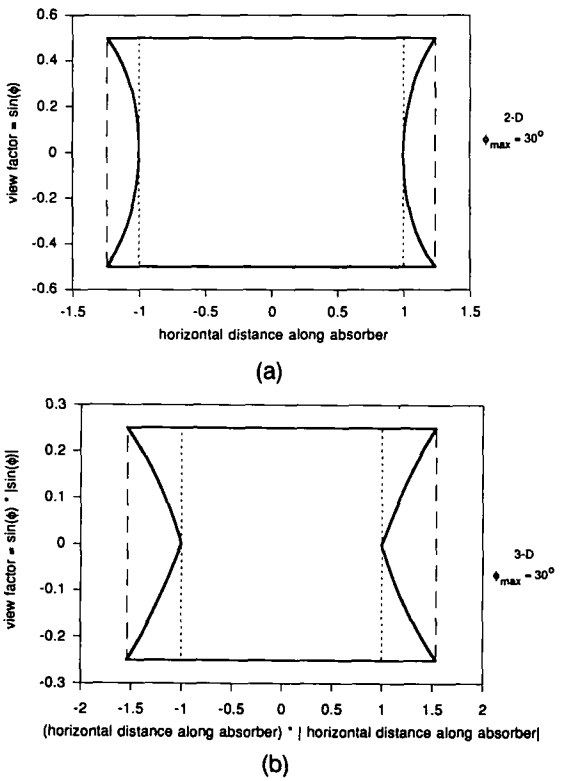

Fig. 8. Phase space region (view factor vs. spatial extent) occupied by radiation focused onto a flat absorber from a (a) 2-D and (b) 3-D parabolic reflector, with the conventional absorber placement in the parabola's focal plane. Étendue is the area within the curve. Smaller and larger rectangular areas, indicated with broken lines, show the extreme designs for secondary CPCs, as discussed in Appendix A. One unit is the radius of the minimum size absorber. $\phi_{max} = 30°$.

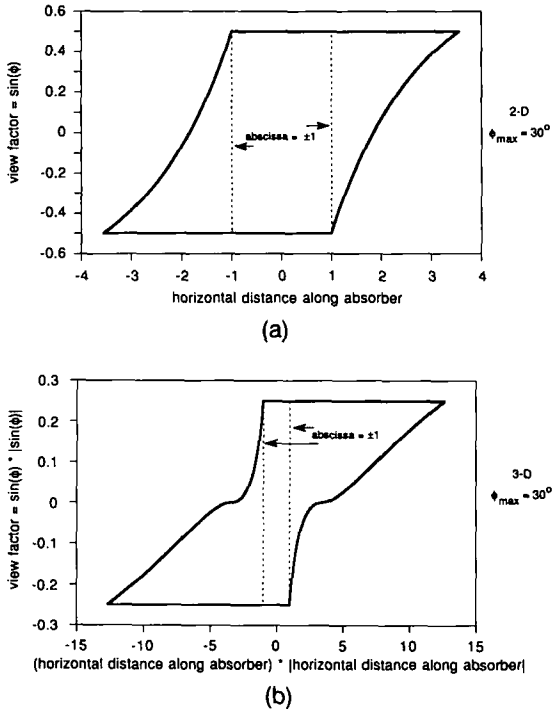

Fig. 9. Phase space region occupied by radiation focused onto a flat absorber from a (a) 2-D and (b) 3-D parabolic reflector, with the new absorber placement for TERC design. One unit is the radius of the minimum-size absorber. $\phi_{max} = 30°$.

"precisely" we mean no more, since this would increase the phase space volume and decrease the concentration; and no less, since this would reduce the accepted radiation and decrease collection efficiency.

The edge-ray principle of nonimaging optics[1]is the guiding tenet for the design of an ideal secondary. Edge rays are all points at the rim of the occupied phase space region. The local slope of a reflector can be selected so that an incident edge ray is also reflected as an edge ray. However this works only if there is *exactly* one edge ray incident, and exactly one edge ray desired, on each point of the reflector. As can be seen from Fig. 8, there are *two* edge rays at the outer parts of the absorber. This precludes introduction of an *ideal* secondary concentrator there.

It is precisely for this reason that we have proposed displacement of the absorber from the focal plane toward the primary, with a construction strategy for a new type of secondary as detailed in section 3. The phase space region occupied by rays incident on the new displaced absorber plane is shown in Fig. 9 (for the specific case of $\phi_{max} = 30°$, and recall the qualification for the interpretation of Fig. 8b, which also pertains to Fig. 9b). The relation between spatial and angular coordinates is then

$$\mathscr{X}(\phi) = 2p(\phi) \quad \text{2-D} \tag{A2a}$$

$$\mathscr{X}(\phi) = \pi p(\phi)|p(\phi)| \quad \text{3-D} \tag{A2b}$$

where

$$p(\phi) = 2f\tan(\phi/2)\tan(\phi \pm \theta_s) \times \left[1 + \frac{1}{\tan(\phi)} - \frac{L}{2f\tan(\phi/2)}\right] \tag{A2c}$$

and the vertical displacement L of the absorber is given by eqn (11). Note that the phase space plot now depends on parabolic extent ϕ_{max} via L.

A key observation is that the new configuration results in a single-valued contour in $\mathscr{X}$, consistent with the requirement of the edge-ray principle. Namely, there is a one-to-one correspondence between location on the primary and points on the secondary (for the TERC construction described in section 3) as dictated by the edge rays.

APPENDIX B: TERC DESIGNS BEYOND THE LIMIT OF STRICT VALIDITY

As noted in subsection 3.2, at parabola rim half-angles above the value determined from eqn (12) (e.g., 36.6° at $\theta_s = 0.010$ radian), the TERC construction strategy fails because the edge rays that establish a minimum radius in the (displaced) absorber plane no longer originate from the parabola's rim ($\phi = \phi_{max}$). A phase space plot [based on eqn (A2)] reveals this problem in the form of edge rays striking the (displaced) absorber plane at positions *smaller* than the minimum size absorber. Namely, a TERC designed for maximum concentration cannot map all rays from the primary into the minimum absorber area, which results in an inconsistent solution. Figure 10 illustrates this point for $\phi_{max} = 45°$.

A compromise solution is described in subsection 3.2, in which one oversizes the absorber (i.e., sacrifices concentration) in order to collect all rays from the primary. Fortunately, this compromise solution results in small sacrifices in concentration up to reasonably large parabola rim angles (because the problematic phase-space area in Fig. 10 is a small fraction of the total area). Plots of achievable concentration (at maximum collection efficiency) and collection efficiency (at maximum concentration) are presented in Figs. 6 and 7, respectively.

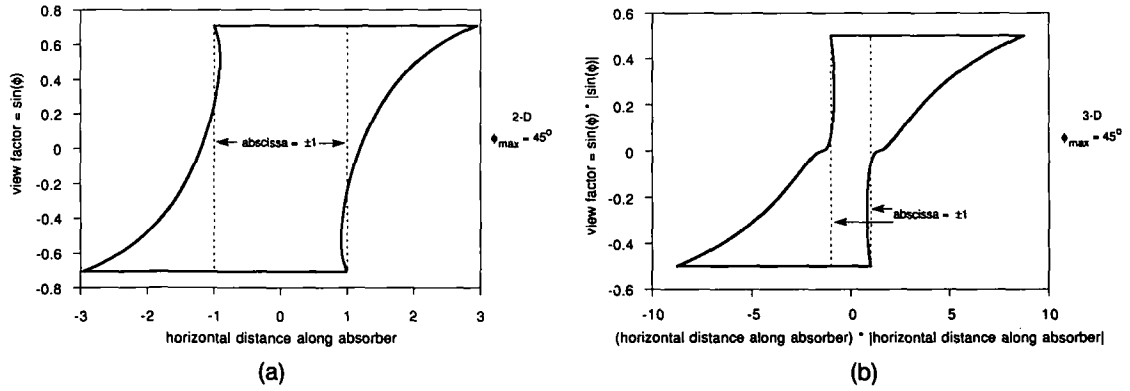

Fig. 10. Phase space region for the new absorber placement for TERC design in (a) 2-D and (b) 3-D, but for $\phi_{max} > \phi^* = 36.6°$. Note that edge rays strike the absorber plane at positions smaller than the radius of the minimum-size absorber. One unit is the radius of the minimum-size absorber. $\phi_{max} = 45°$.